LA-UR-21-30732
Approved for public release; distribution is unlimited.

Title: TRUST Nonlinear Dynamics (ND) Report

Author(s): Lum, Sheera Shelby
Brindley, Kyle Andrew

Intended for: Report

Issued: 2021-12-02 (rev.1)

TRUST Nonlinear Dynamics (ND) Report

Release FY21.1.1

Sheera S. Lum, Kyle A. Brindley

Nov 03, 2021

CONTENTS

1 Introduction **3**

2 Experiments **5**
2.1 Testbed Assembly 5
2.2 Methodology 6

3 Model **7**
3.1 Geometry 8
3.2 Mesh 11
3.3 Boundary Conditions 13
3.4 Loading Conditions 13
3.5 Materials 13
3.6 Interactions and Constraints 13
3.7 Analysis 14

4 Results & Discussion **15**

5 Future Work **17**

6 Conclusions **19**

7 Acknowledgments **21**

Bibliography **23**

The objective of the Delivery Environments (DE) Testbeds to Reduce Uncertainties in Simulations and Tests (TRUST) work package is to quantify and help increase confidence in specific areas of computational and experimental capabilities that are applicable to current and future delivery environments. More complete quantification of confidence in experimental and computational capabilities and the sufficient increase of confidence in those capabilities is critical to improving weapons engineering design, qualification, and assessment efforts that are critical to the current and future stockpile. Staff development will include cross-discipline training to provide engineers with experience in both numerical simulations and experimental methods. This work will use and provide feedback on analysis tools and experimental results databases for efficient and responsive engineering which are currently under development: engineering common model framework (ECMF), engineering quantification of margins and uncertainties (EQMU), and the test information management system (TIMS).

TRUST includes four testbeds and their associated engineering analysis baseline models (EABMs):

1. contact thermal conductivity (CTC)
2. nonlinear dynamics (ND)
3. sensors in environments for accelerometers (SEA)
4. sensors in environments for fiber optic displacement gages (SEFOD)

The TRUST work package contains three testbeds and their associated engineering analysis baseline models (EABMs):

1. contact thermal conductivity (CTC)
2. nonlinear dynamics (ND)
3. sensors in environments (SE)

CHAPTER

ONE

INTRODUCTION

Nonlinear behavior of a system under dynamic loading conditions can sometimes be directly caused by nonlinear material properties. Such behavior is present in many components of interest to the Weapons division at Los Alamos National Laboratory (LANL). The TRUST nonlinear dynamics testbed was developed with the aim of investigating and building on current dynamic modeling capabilities. Several subject matter experts (SMEs) have expressed interest in fabricating a test setup that is capable of dynamically loading a compliant material stackup, focusing on the conceptual design shown in Figure 1.1 [1].

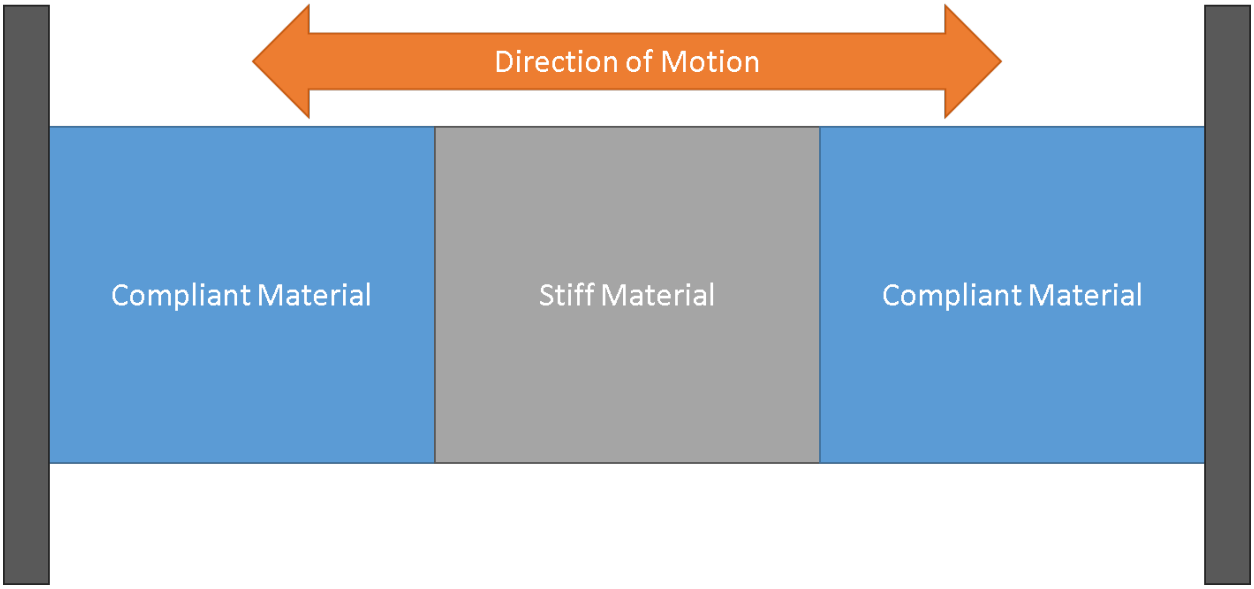

Fig. 1.1: Schematic for the conceptual design of the dynamics testbed

While keeping in mind the main goals of TRUST, the testbed was iteratively designed to mitigate sources of uncertainty such as asymmetry. The final configuration of the testbed design consists of a vertical material stackup where a stiff material is placed in compression between two relatively more compliant materials like the hyperelastic foam stackup shown in Figure 3.1. This testbed addresses both the dynamic response of nonlinear materials as well as preload sensitivity within material stackup assemblies [1].

Using a voltage input, uniaxial acceleration will be applied to the assembly along the central axis of the material stackup. Applying a simple axial vibration to the testbed provides a direct approach in investigating the dynamic behavior of the material stackup.

The testbed's schematic design allows areas of uncertainty outside the feature of interest (i.e. dynamic behavior of material) to be minimized. The design permits multiple stackup configurations to be incorporated as desired, allowing the testing of a variety of material combinations to be executed using the same testbed [1].

CHAPTER

TWO

EXPERIMENTS

This section summarizes the TRUST dynamics testbed assembly and test procedure. A detailed description of the test setup and methodology is provided in [2].

2.1 Testbed Assembly

Figure 2.1 shows a labeled cross-section view of the TRUST dynamics testbed. The baseplate provides a stable means for attaching the testbed to the shaker. The spacer ensures sufficient clearance is always maintained between the baseplate accelerometers and the accelerometer mounting blocks, six (6) of which were were placed equidistant about the loading axis as shown in Figure 2.1. These blocks were attached to the testbed mass to provide stable accelerometer stations. Six (6) accelerometers were attached to the testbed mass to record the mass's dynamic behavior. Two (2) additional accelerometers were attached to the baseplate to record the dynamic behavior of the shaker. All eight sensors were triaxial so that any out-of-axis behavior within the system was recorded. Low-stiffness components (i.e. wave springs and foams for linear and nonlinear cases, respectively) provide the high relative compliance needed to observe the dynamic behavior of the testbed mass. The through bolt shown in Figure 2.1 was used to preload the testbed by twisting down a nut at the top of the bolt, using a load cell to monitor the load value both prior to and during testing. The upper plate evenly distributed the preload across the material stackup to promote symmetric loading.

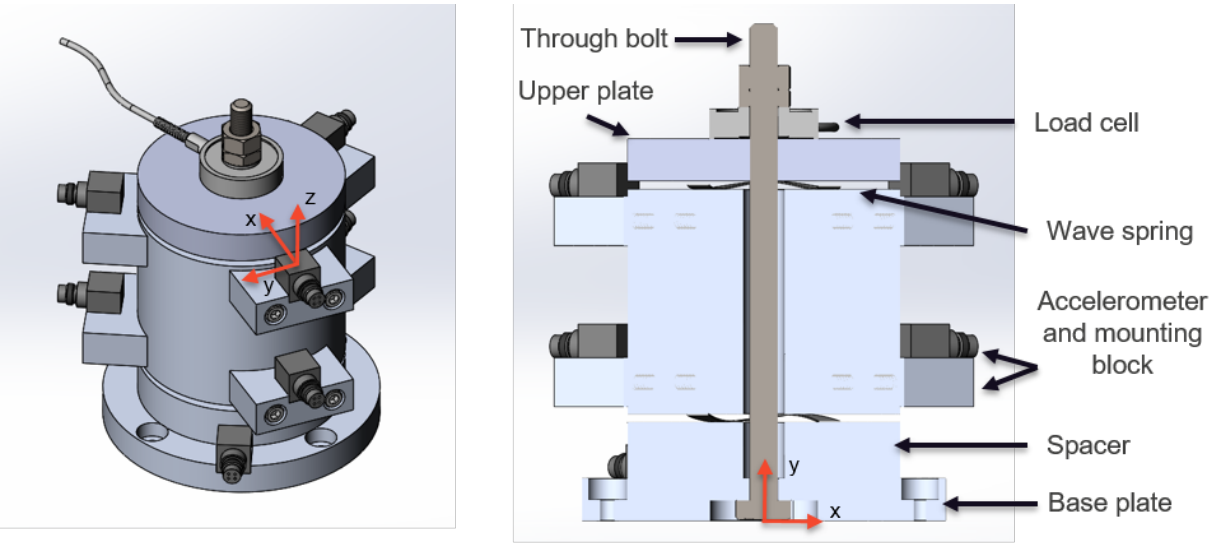

Fig. 2.1: Isometric (left) and cross-sectional (right) views of the dynamics testbed. The coordinate system (CS) on the left denotes the local CS for each accelerometer, while the one on the right is the testbed assembly reference CS for the 2D axisymmetric model.

2.2 Methodology

The testbed was attached to the shaker and the sensor systems were set up as described in [2]. Test parameters were input into LabView signal processing software, focusing on the extraction of accelerometer time histories in x-, y- and z-directions and load cell and shaker time histories [3, 4]. Each accelerometer was attached to the testbed such that their z-directions were parallel to the primary loading (i.e. vertical) direction. An example of the local coordinate system (CS) for each accelemerometer can be seen in Figure 2.1, noting that the positive x-direction points radially inward towards the testbed center. A sinusoidal voltage was defined for the shaker input, setting units to mV. Depending on the test sequence, the input profile was defined as single tone, stepped-sine, or white noise [3].

Test iterations spanned 30-90 s, and time histories for all sensors were collected at a rate of at least twice the maximum expected frequency imparted to the system. Initially, determining the frequency range was done iteratively, noting the voltage input required to achieve a desired shaker frequency. Time histories were written to Technical Data Management Streaming (TDMS) [5] file format, saved to a usable Excel format for future post-processing, and uploaded to the Test Information Management System (TIMS) [6, 7, 8]. The frequencies of the system were extracted from these saved time histories and used to determine the maximum frequency experienced by the system [3]. Tests were modified to achieve a range of 5-2000 Hz, which was the frequency range of interest laid out by TRUST [1].

CHAPTER

THREE

MODEL

The TRUST dynamics model aims to simulate the linear and nonlinear dynamic behavior of the material stackup system within the TRUST dynamics testbed shown in Figure 3.1. The 2D axisymmetric model employs two configurations: a spring-mass-spring stackup and a foam-mass-foam stackup. The former configuration serves to verify the testbed's linear behavior without the presence of nonlinear/hyperelastic materials as well as validate the model's linear predictive capabilities. The aim for the latter configuration is to validate the model against a nonlinear dynamic setup (i.e. a system containing hyperelastic materials). Physical testing was and will continue to be used to verify the linear testbed setup as well as validate the 2D axisymmetric model, which will be precompressed and excited via uniaxial random acceleration.

The model implements a quasi-staic Abaqus/Standard [9] implicit analysis step to preload the testbed, followed by a modal analysis step to extract the resonant frequencies from the model.

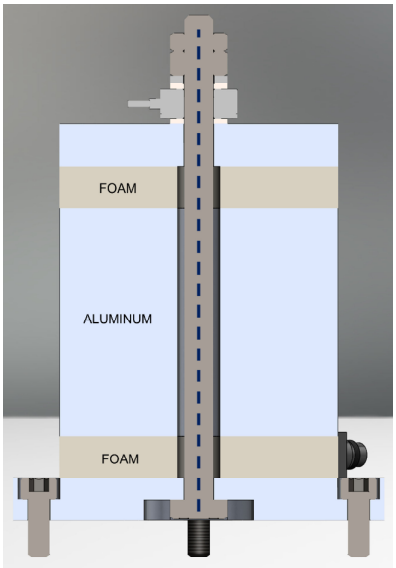

Fig. 3.1: Cross-section of the TRUST dynamics testbed employing a foam-mass-foam stackup configuration.

The geometry and mesh for each part in the assembly were generated using Cubit [10] journal files [11]. The Engineering Common Model Framework (ECMF) [12] allows a model's geometry and mesh build to be easily parameterized for use in Cubit by initially defining all variables within a baseline configuration file before building the parts [13]. Taking advantage of this feature, a base set of geometry parameters was defined and read into Cubit as variables to construct part geometry.

3.1 Geometry

An axisymmetric model was implemented to take advantage of the testbed's symmetry. The axisymmetric geometry was constructed based on the nominal dimensions provided in the nonlinear dynamics testbed drawing [14]. For the load cell and load washer geometry, dimensions were taken from drawings provided by PCB Piezotronics [15]. All part geometry was modeled using Cubit meshing software, saving the geometry for each part to individual Cubit (.cub) files. The position in the testbed assembly was also defined for each part prior to export, using the coordinate system shown in Figure 2.1 as the reference CS.

3.1.1 Baseplate

The axisymmetric baseplate geometry was based on Drawing 102Y233276 of the testbed drawing [14], the isometric view of which can be seen in Figure 3.2(a). The geometry was defeatured by removing the bolt holes for mounting the part to the shaker. All nonaxisymmetric features were either omitted or simplified. The axisymmetric representation of the baseplate was placed in Figure 3.2(b), noting that the defeatured, 3D representation of the baseplate geometry could be fully restored by revolving the 2D geometry 360 degrees about its symmetry axis.

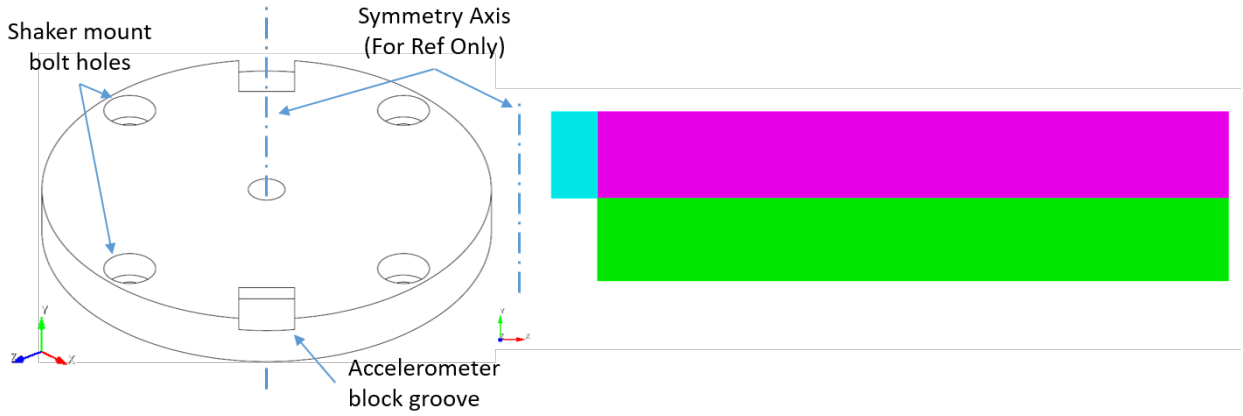

Fig. 3.2: From left to right: (a) Isometric view of the baseplate. (b) (Scale increased for visibility) Axisymmetric representation of the partitioned baseplate geometry.

3.1.2 Center Mass

The nominal dimensions found in Drawing 102Y233278 from the testbed drawing [14] were used to form the axisymmetric geometry of the center mass. All threaded holes such as those shown in Figure 3.3(a) and other nonaxisymmetric features were omitted. The final axisymmetric representation of the center mass was placed in Figure 3.3(b).

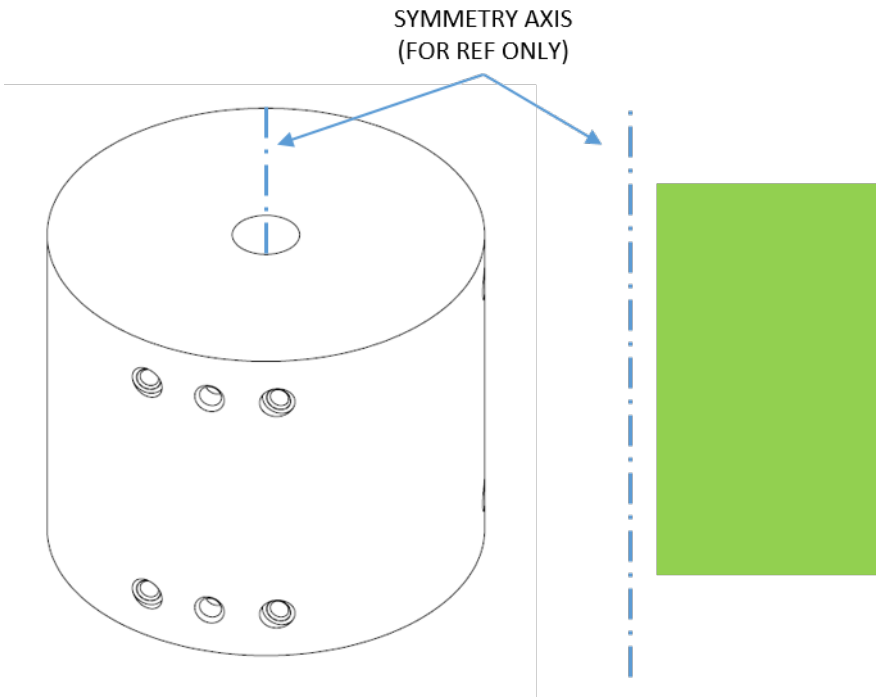

Fig. 3.3: From left to right: (a) Isometric view of the center mass. (b) (Not to scale) Axisymmetric representation of the center mass geometry.

3.1.3 Spacer and Upper Plate

Given their similarities, the axisymmetric geometries for both the spacer and upper plate were constructed in much the same way, taking nominal dimensions from drawings 102Y233277 and 102Y233279 from the testbed drawing [14] for the spacer and upper plate, respectively. Each part is based on three nominal dimensions (i.e. outer diameter, inner diameter, and thickness); no additional defeaturing was necessary. The original geometry of both parts was sliced in half along the part's thickness to obtain their 2D axisymmetric geometries. As an example, an isometric view of the spacer along with its 2D representation were placed in Figure 3.4.

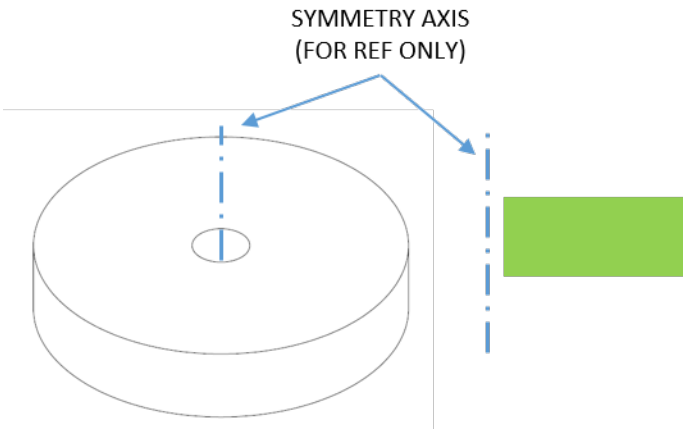

Fig. 3.4: From left to right: (a) Isometric view of the spacer. (b) (Not to scale) Axisymmetric representation of the spacer geometry.

3.1.4 Load Cell Assembly

The load cell assembly supplied by PCB Piezotronics is composed of the load cell and two (2) washers placed above and below the load cell, which can be seen in Figure 3.5(a). Referencing the nominal drawing dimensions provided by the manufacturer [15], the axisymmetric representation of each part was created. W-13 was told by PCB Piezotronics to assume the load cell material was uniform throughout, thus allowing the part to be represented as a single component. All nonstructural features such as chamfers were omitted from the geometry for both the load cell and washers. Like that of the spacer and upper plate, the axisymmetric geometries for both the load cell and washers were visualized by slicing each part in half along its thickness. The final 2D axisymmetric representation of the assembly can be seen in Figure 3.5(b).

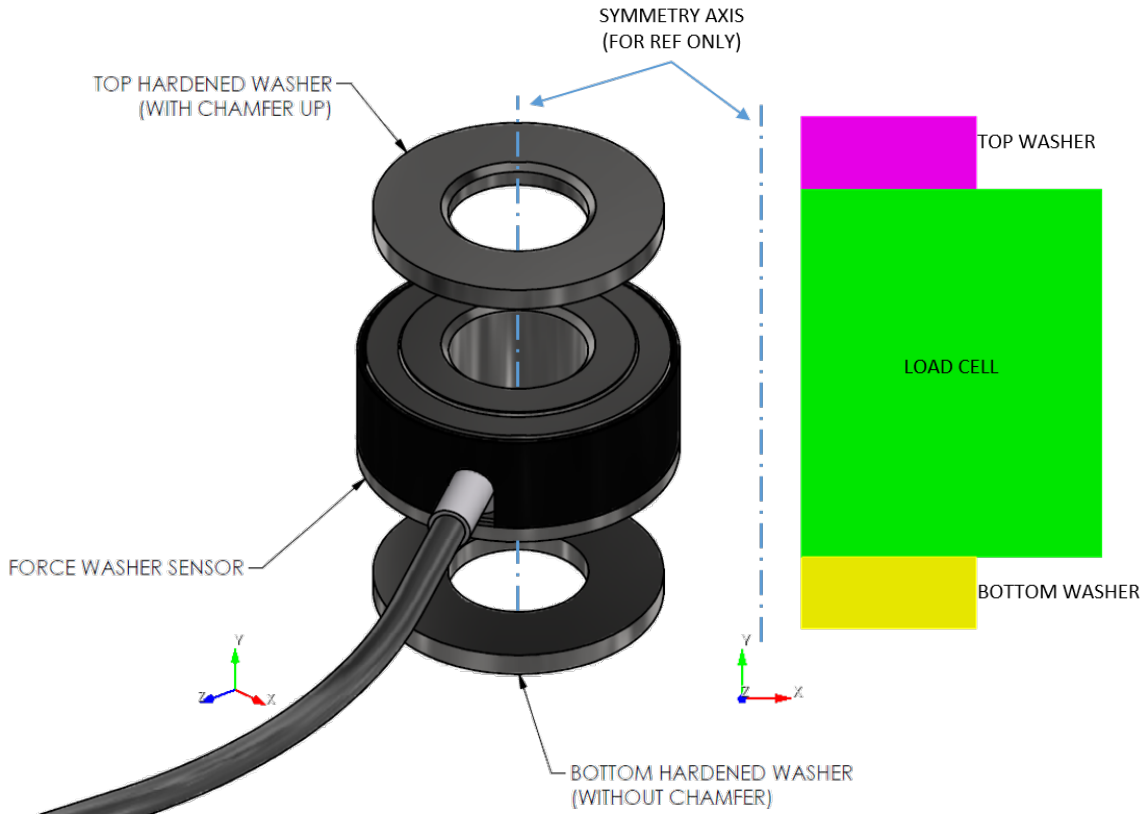

Fig. 3.5: From left to right: (a) Exploded view of the load cell assembly. (b) (Scale increased for visibility) Axisymmetric representation of the load cell assembly.

3.1.5 Bolt

The bolt shank, head, and nut were modeled as one part using nominal part dimensions provided in the parts list located in Drawing 102Y2332765 from the testbed drawing [14]. Bolt threads were excluded so that the geometry could be modeled as axisymmetric. The bolt shank length was calculated by adding up the nominal thicknesses of the parts preloaded by the bolt. A cross-sectional view of this stackup can be seen in Figure 2.1.

As shown in Figure 3.6, a partition cut was made through the bolt shank so that a preload definition could be applied to the bolt during the Abaqus loading step discussed in *Loading Conditions*.

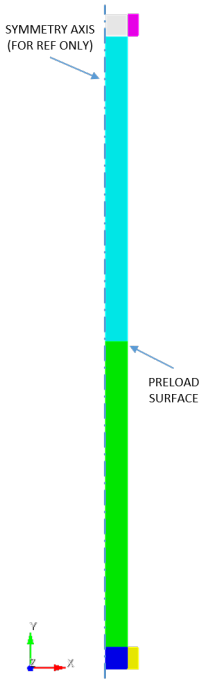

Fig. 3.6: Axisymmetric representation of the bolt.

3.1.6 Spring

Because the spring geometry is non-axisymmetric (see Figure 2.1, the wavesprings were modeled as axial springs, whose lines of action run parallel with the axial direction (y-direction) of the testbed.

3.2 Mesh

As depicted by the different colored regions shown in figures 3.2(b) and 3.6, the axisymmetric geometry was partitioned to maximize mesh quality. Partitioning not only improves the mesh quality but also eliminates the need for using an unstructured mesh, which can be more distorted and computationally more expensive. All partitioned volumes were imprinted and merged with their respective parts. Imprinting ensures all nodes associated with a single part will align across the partitioned regions, while merging removes redundant nodes that arise from partitioning.

Part meshes were created in Cubit by importing the geometry described in *Geometry*, followed by exporting meshes as 2D Abaqus input files. The part meshes were controlled using a global surface seed size of 1 mm, which was determined to be a sufficient seed size based on prior convergence studies. Like the geometry parameters, the seed was assigned as a Cubit variable, allowing the model user to define their desired element size at the configuration file level.

Because Cubit does not have the option to select an axisymmetric-compatible element type, the input files for each part were automatically revised after export by specifying this modification at the configuration file level [16]. Each mesh was reassigned to have continuum 4-node bilinear axisymmetric elements with reduced integration and hourglass control (CAX4R). Reassigning element type had no effect on the original geometric mesh quality.

Within Cubit, there are three main types of sets used to group nodes and elements: sidesets, nodesets, and blocks. Cubit sidesets are equivalent to Abaqus element sets upon exporting a Cubit mesh as an Abaqus orphan mesh. Similarly, Cubit nodesets correspond to node-based sets in Abaqus. Blocks are composed of a group of elements and are particularly useful for exporting only the elements forming a single part. Using these features, elements corresponding

to a single part were assigned to a unique element set so that each respective set could be referenced when instancing the part in Abaqus. Additionally, node sets were assigned to surfaces that would be coupled to the connector elements as well as to surfaces that would be assigned boundary conditions.

Each of the parts were assembled in the Abaqus axisymmetric model by instancing each part mesh within the same Abaqus input deck. The axisymmetric meshed assembly can be seen in Figure 3.7.

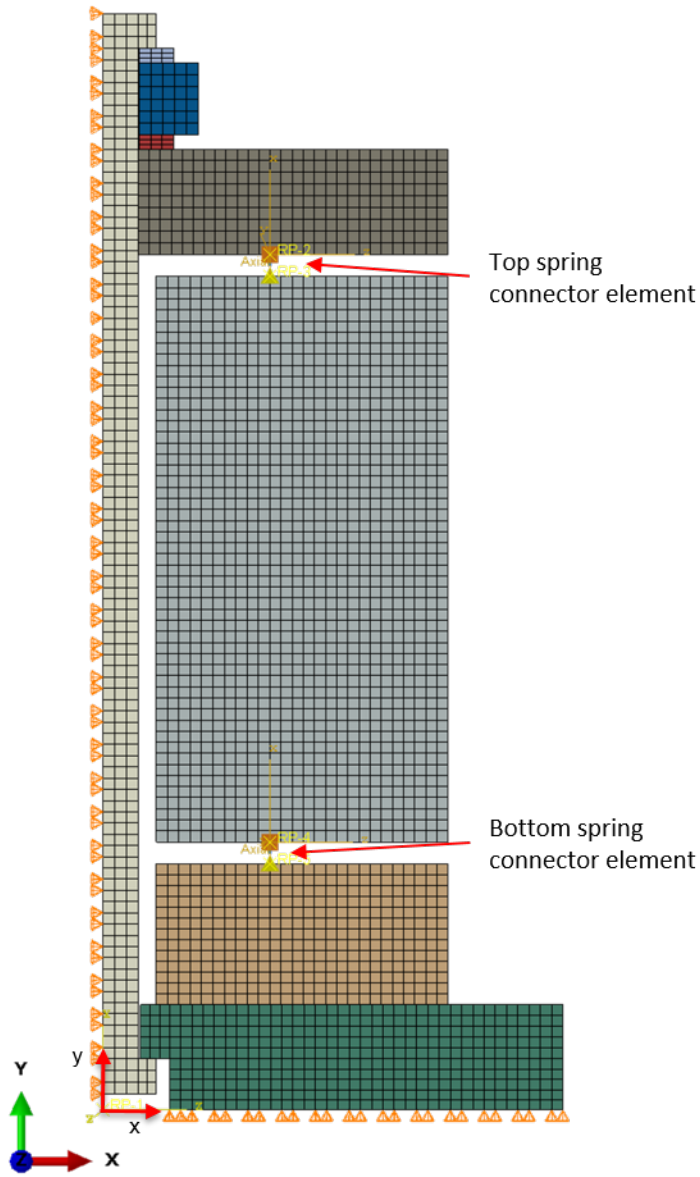

Fig. 3.7: Meshed model for the TRUST nonlinear dynamics testbed. The red CS denotes the assembly origin.

Shown in Figure 3.7, a CONN2D2 connector element was applied to both springs, which mimics linear spring stiffness and is compatible with both Abaqus/Standard implicit and Abaqus/Explicit simulations. Each connector element was placed ~15 mm from the symmetry axis, which equates to the contact region of the wavesprings in the physical testbed.

3.3 Boundary Conditions

To prevent nonphysical translations, all nodes coincident with the symmetry axis were fixed in the radial direction (x-direction). To prevent rigid body translation, the bottom of the baseplate was fixed in the axial direction (y-direction).

3.4 Loading Conditions

A uniform gravitational acceleration in the negative y-direction was applied to the entire model. The load was applied linearly over the course of the preload step, ranging from 0 to $9.81 m/s^2$.

During the same step, a bolt load was applied normal to the preload surface shown in Figure 3.6. The load was applied linearly over the course of the preload step time from 0 to $222N$ (~ $50lbs$).

3.5 Materials

The baseplate, spacer, center mass, and upper plate of the testbed were fabricated from 6061-T6 aluminum alloy, which was modeled using material properties from the Metallic Materials Properties Development and Standardization (MMPDS) handbook [17]. For the bolt, a steel alloy was used for the material definition [18]. For the load cell assembly (load cell and load cell washers), a material model consistent with 440 stainless steel hardened to a Rockwell Hardness (RC) of 58-60 was assigned to the part instances [19]. The load cell material was recommended by its respective supplier (PCB Piezotronics). The material properties assigned to the part instances within the model were placed in Table 3.1.

Table 3.1: Material parameters used for the nonlinear dynamics axisymetric model

Material	Density $tonne/mm^3$	Young's Modulus MPa	Poisson's Ratio	Yield Stress MPa	Part
6061-T6 Al	2.71263E-09	6.82581E+04,	0.33	234.422	Baseplate, spacer, center mass, upper plate
Alloy Fe-9Ni	7.83331e-9	2.04039E+05	0.31	1.25422E+03	Bolt
SS 440C	7.79936e-9	1.99750E+05	0.28	1.89048E+03	Load cell assembly

3.6 Interactions and Constraints

A general contact definition was applied to the model, assuming frictionless tangential behavior (for the modal analysis step) and hard pressure-overclosure.

The end nodes of the spring connector elements were coupled to the contacting surfaces using a continuum distributing coupling definition. A uniform weighting method was applied to each coupling definition and all degrees of freedom (i.e. U1, U2, and UR3) were constrained.

3.7 Analysis

A static analysis step was used for preloading the bolt, and geometric nonlinearities were also considered. Because the application of the step was defined as quasi-static, the amount of time over which the step occurred had no effect on the output. Thus, a convenient step value time of 1 second was chosen for the step duration.

Following the preload step, an Abaqus linear perturbation analysis was applied to the model to extract the modal frequencies, using a Lanczos eigensolver and requesting the first three modal frequency values as output. All boundary conditions applied in the preload step were maintained for the duration of the modal study.

A parametric study was performed by varying the spring stiffnesses across a range of values, with the lower bound pertaining to the nominal spring stiffness determined from Instron compression tests performed by E-1. The two-step analysis was repeated for each parameter set of the study, assigning the same stiffness to the two spring elements and recording the resultant modal frequencies.

CHAPTER

FOUR

RESULTS & DISCUSSION

Axial compression testing of four of the wavespring samples indicated that the nominal stiffness of the springs was close to 200 N/mm (1142 lbf/in). The uncertainty associated with this nominal stiffness is not discussed in this report. Using the nominal stiffness as the lower bound of the parametric study, the modal analyses were executed over a range of 200 to 400 N/mm. The primary purpose of the parametric study was to verify that the model behaved predictably.

The first two modal frequencies as a function of spring stiffness can be seen in Figure 4.1. Though the first three frequency modes were requested as output, the third mode exceeded the frequency range of interest (2000 Hz) and was thus omitted. As anticipated, both modal frequencies follow a clear trend as the spring stiffness is increased.

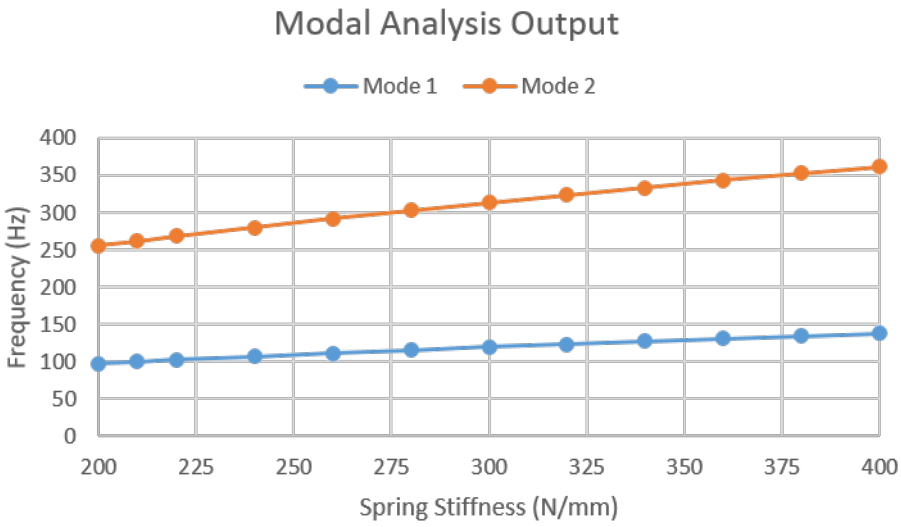

Fig. 4.1: Resultant frequency modes that arise when the spring stiffness is modified.

When comparing the analysis results with the physical testbed results discussed in [3], modal frequencies 1 and 2 from the Abaqus analysis are notably lower than modes 1 and 2 estimated from performing modal testing on the dynamics testbed. Interestingly, mode 2 from the analysis is comparable to the first frequency mode from the physical testbed.

CHAPTER

FIVE

FUTURE WORK

As a continuation of TRUST efforts using the dynamics testbed, the dynamic behavior of a stackup configuration containing a nonlinear material will be investigated. Samples of varying thicknesses and porosities for SX358 foam fabricated by MST-7 will replace wave springs in the stackup assembly, and tests will be executed using a process similar to that described in [3]. The test results will be uploaded to TIMS, post-processed, and used to validate the testbed model described in *Model*. To further explore modeling capabilities, additional experiments will be executed with both increased environmental uncertainty and materials that have not yet been well-characterized. Resultant data will be fed into the model to identify, measure, and propagate any resulting uncertainty to quantities of interest in simulation predictions. Analysis techniques and results will be documented in a final report.

To better represent the testbed structure as well as the effects of accelerometer placement, a 3D model may also be created and validated. In addition to providing a more realistic testbed representation, a 3D model will also be beneficial in verifying the intended uniaxial behavior of the testbed in conjunction with the experimental measurements.

CHAPTER

SIX

CONCLUSIONS

Through the nonlinear dynamics testbed, TRUST analysts developed a testbed and test method that quantifies W-13's current material model predictive capabilities in dynamic environments. With most hyperelastic materials calibrated using quasi-static test data, their behavior in a dynamic environment has not been as well-characterized. Incorporating a material stackup using well-known linear materials was recently concluded to assess the behavior of the testbed. The knowledge gained from this study will be used to modify the model as needed until the model aligns with that of the experimental results.

The data discussed in *Results & Discussion* shows that the dominant modal frequencies for the linear testbed are notably different than the values approximated for the dynamics model. This discovery indicates that further investigation is necessary to understand what elements are contributing to this disparity in behavior. Possible solutions include performing sensitivity studies on the material properties in addition to the wavespring stiffnesses or increasing the overall model fidelity. Both approaches will be considered to determine what is causing the frequency response discrepancy between the testbed and model.

Once the predictive capabilities of the linear dynamics model are validated against the experimental behavior, efforts will transition to completing nonlinear dynamics testing, replacing linear elements with SX358 hyperelastic foam samples. Results from nonlinear testing will be compared to the model to observe how well the model predicts nonlinear material behavior in a dynamic environment.

CHAPTER

SEVEN

ACKNOWLEDGMENTS

The work discussed in this report was made possible through cross-collaborative efforts among groups E-1, NSEC, and W-13. Testbed design, fabrication, and testing were completed largely due to members' efforts within E-1, with Elizabeth Martinez performing much of the testing and instigating all refabrication requests. Peter Meyerhofer from NSEC produced the code required for test execution. Additional thanks to W-13 members for providing expert guidance on carrying out analysis and testing efforts.

BIBLIOGRAPHY

[1] Kyle A. Brindley and Antranik A. Siranosian. Single feature testbeds to reduce uncertainties in simulations and tests. Technical Report LA-UR-19-29860, Los Alamos National Laboratory, Los Alamos, New Mexico, USA, 2019.

[2] Ryan Maki and John Morales Garcia. Trust testing procedure documentation. Technical Report LA-UR-20-27402, Los Alamos National Laboratory, Los Alamos, New Mexico, USA, 2020.

[3] Peter Meyerhofer and Elizabeth Martinez. Trust nonlinear dynamics testbed assessment. Technical Report LA-UR-21-29338, Los Alamos National Laboratory, Los Alamos, New Mexico, USA, 2021.

[4] Peter Meyerhofer. Trust_nd_labview_code_lfs. 2021. URL: https://git.lanl.gov/pmeyerhofer/trust_nd_labview_code_lfs (visited on 2021-10-26).

[5] National Instruments. The NI TDMS file format. June 2021. URL: https://www.ni.com/en-us/support/documentation/supplemental/06/the-ni-tdms-file-format.html (visited on 2021-10-26).

[6] Los Alamos National Laboratory. Test information management system (TIMS). 2020. URL: http://miweb/mi/index.aspx (visited on 2020-09-04).

[7] Bartlomiej Benedikt. Test information management system. report fy 2020 and fy 2021. Technical Report LA-UR-21-29767, Los Alamos National Laboratory, Los Alamos, New Mexico, USA, September 2020.

[8] Elizabeth Martinez, Peter Meyerhofer, and Sheera Lum. TRUST: nonlinear dynamics testbed (TRUST: ND). 2021. URL: http://grantami.lanl.gov/mi/index.aspx?profileKey=MI_TIMS_v10.0 (visited on 2021-10-26).

[9] Dassault Systemés Simulia Corporation. Abaqus 2019. 2019. Providence, RI, USA.

[10] Sandia National Laboratories. Cubit 15.5. 2019. Albuquerque, New Mexico, USA.

[11] Kyle Brindley, Thomas LeBrun, Sheera Lum, and Manuel Vega. Trust. 2021. URL: https://re-git.lanl.gov/aea/models-and-simulations/trust (visited on 2021-10-26).

[12] Los Alamos National Laboratory. Engineering common model framework (ECMF). 2021. URL: https://aea.re-pages.lanl.gov/python-projects/ecmf/master/ (visited on 2021-09-21).

[13] Scott Ouellette, Prabhu Khalsa, Kyle Brindley, Thomas LeBrun, Isaac Salazar, Brandon Stone, and Trevor Tippetts. The engineering common model format (ecmf): a new vision on model development best practices for enhanced engineering analysis collaboration. Technical Report, Los Alamos National Laboratory, Los Alamos, New Mexico, USA, January 2020.

[14] Los Alamos National Laboratory. Nonlinear dynamics testbed drawing. 2021. URL: https://aea.re-pages.lanl.gov/models-and-simulations/trust/master/nd-html-model-guide.html#testbed-drawing (visited on 2021-09-23).

[15] PCB Piezotronics. Drawing lt30776. 2021. URL: https://www.pcb.com/contentStore/docs/pcb_corporate/forcetorque/products/drawing/pdf/lt30776-h.pdf (visited on 2021-09-23).

[16] Los Alamos National Laboratory. *Engineering Common Model Framework (ECMF)*. Los Alamos, New Mexico, USA, 2020. ECMF documentation: Configuration File API: Configuration file elements: SolverPrep. URL: https://aea.re-pages.lanl.gov/python-projects/ecmf/master/config_api.html (visited on 2021-09-21).

[17] MMPDS-13 Database. 6061, t6, extruded rod, bar, shapes, thickness: 1.001 to 6.501 in, area: up to 32.001 sq in, ams 4150, a basis. Record History Guid:1025020a-a801-2301-0032-310650000100, Record Version Guid:1025020a-a801-2301-0032-310650000102.

[18] "Intermediate Alloy, Fe-9Ni-4Co-0.20C Steel, Quenched & Tempered," V.X, Database: MaterialUniverse, 5.51.1m_Dec2018, Granta Design.

[19] "Stainless Steel, Martensitic, AISI 440C, Tempered at 316°C," V.X, Database: MaterialUniverse, 5.51.1m_Dec2018, Granta Design.